

## The pore structure of Sierpinski carpets

This article has been downloaded from IOPscience. Please scroll down to see the full text article.

2001 J. Phys. A: Math. Gen. 34 8751

(<http://iopscience.iop.org/0305-4470/34/42/303>)

View [the table of contents for this issue](#), or go to the [journal homepage](#) for more

Download details:

IP Address: 171.66.16.98

The article was downloaded on 02/06/2010 at 09:21

Please note that [terms and conditions apply](#).

# The pore structure of Sierpinski carpets

A Franz<sup>1</sup>, C Schulzky<sup>2</sup>, S Tarafdar<sup>3</sup> and K H Hoffmann<sup>1</sup>

<sup>1</sup>Institut für Physik, Technische Universität, D-09107 Chemnitz, Germany

<sup>2</sup>Department of Applied Mathematics, The University of Western Ontario, London, Ontario, Canada N6A 5B7

<sup>3</sup>Condensed Matter Physics Research Centre, Jadavpur University, Calcutta 700032, India

Received 22 November 2000, in final form 27 July 2001

Published 12 October 2001

Online at [stacks.iop.org/JPhysA/34/8751](http://stacks.iop.org/JPhysA/34/8751)

## Abstract

In this paper, a new method is developed to investigate the pore structure of finitely and even infinitely ramified Sierpinski carpets. The holes in every iteration stage of the carpet are described by a hole-counting polynomial. This polynomial can be computed iteratively for all carpet stages and contains information about the distribution of holes with different areas and perimeters, from which dimensions governing the scaling of these quantities can be determined. Whereas the hole area is known to be two dimensional, the dimension of the hole perimeter may be related to the random walk dimension.

PACS numbers: 05.45.Df, 61.43.Hv, 61.43.Gt, 81.05.Rm, 05.40.Fb

## 1. Introduction

Porous materials, such as aerogels, sedimentary rocks, bio-membranes, corals and sponges, form a large class of real fractals around us. The pore structure plays an important role in determining many properties of such materials. The pore structure is extremely complicated, and identifying features which can be associated with any property is a major problem. The simplest quantity is *porosity*, which is the fraction of pore volume, compared to the total sample volume. However, the only information on porosity is inadequate to understand, for example, transport properties of a porous material. In the present paper we investigate further details of the pore structure of a deterministic fractal and show that the interface area of the pores is another important characteristic, which can be used to give an approximate estimate of dynamic properties such as diffusion.

An ideal fractal, of course, cannot have a definite porosity because the porosity in this case would tend to 1 or 0 as we explain later. We are concerned here with real systems, which have a macroscopic density or porosity on a large scale ( $\sim$ mm), but on an intermediate scale ( $\sim\mu$ m) are fractal, whereas at a small length scale ( $\sim\text{\AA}$ ) become homogeneous again.

Porous systems are often modelled by fractal structures, like the Sierpinski gasket or carpets, or the Menger sponge [1, 2]. First, we must clarify which component of the system

is fractal—the solid material or the pore space. Obviously, if one is fractal the other must be compact. Experiments such as x-ray and neutron scattering, or adsorption of gases with different sized molecules, reveal the fractal nature of a real system [1]. Scattering experiments clearly show whether the system is mass-fractal or surface-fractal. The probe (neutron or x-ray photon) sees only the solid material; so the information obtained refers to the solid phase.

For porous rocks, the interface is found to be fractal, so the pore space is fractal, whereas for aerogels, the solid material is fractal. It is possible to model both types of porous media by the same deterministic fractal model by assigning the fractal component to the solid phase in one case and to the pore space in the other. This has been done in [3, 4] for aerogels and sedimentary rocks. We illustrate this in further detail in the next section.

The object of modelling a porous system in such a manner is usually to study some property which depends on the porosity—this may be a transport property, such as diffusivity, electrical or thermal conductivity. It may also be a property dependent on the area of the interface between pore and solid—such as the efficiency of a catalyst or adsorber of a gas or liquid. For these properties the volume of a pore as well as its interface area are very important quantities. Thus, efficient methods to determine pore volumes and surfaces are needed.

This work demonstrates a method for calculating the pore volume and interface area for Sierpinski carpets in two dimensions at any specified stage of iteration. The results can be applied to calculate properties which depend on these properties. We also use this method to show that the size distribution of pore volumes follows a power law with an exponent  $d_f/2$  (as it should) and the interface also follows a power law distribution with a new exponent characteristic of the fractal structure.

## 2. Sierpinski carpets and porosity

Sierpinski carpets are special kinds of self-similar fractals in the plane. They are constructed in the following way: start with a unit square, divide it into  $n \times n$  congruent smaller subsquares and remove  $(n^2 - m)$  of them, corresponding to a given  $n \times n$  pattern called the *generator* of the Sierpinski carpet. Repeat this construction step with all the remaining subsquares *ad infinitum*. The resulting object is a fractal of dimension  $d_f = \log(m)/\log(n)$  [5], called a *Sierpinski carpet*. Further on, we restrict our considerations to connected carpet patterns, i.e. the dark squares of the generator have to be connected by a common edge. An example of such a Sierpinski carpet generator and the second and third iterations of the construction procedure is shown in figure 1.

Sierpinski carpets can be finitely or infinitely ramified. In a *finitely ramified* fractal, any part can be separated from the rest by cutting a finite number of connections. This property can also be checked in the generator as described later.

In order to use Sierpinski carpets as models for porous media, let us consider the white squares as phase 1 and the dark squares as phase 2. If phase 1 is the pore space and phase 2 is the solid phase, then on iteration the pore space goes on increasing and the solid phase decreasing. In this case the solid phase is the fractal. Thus, porosity increases during the iteration: for the example carpet shown in figure 1 the porosity of the generator is  $P_1 = 1 - 11/16 = 5/16$ . In the second stage it is  $P_2 = 1 - (11/16)^2$ . So at the  $i$ th stage the porosity will be  $P_i = 1 - (11/16)^i$  and  $P_i \rightarrow 1$  for  $i \rightarrow \infty$ .

The real material has some definite macroscopic porosity  $P_{\text{mac}}$ . So one can choose a suitable fractal generator and iterate it up to the required stage  $i$  so as to get the right porosity  $P_{\text{mac}}$ . The overall picture of the material is, therefore, as if a fractal unit iterated up to stage  $i$  (the  $i$ th stage ‘iterator’ as it is termed in [6]) is repeated periodically to give a structure homogeneous at length scales  $\gg 1$  [7]. Furthermore, since the smallest building blocks of the

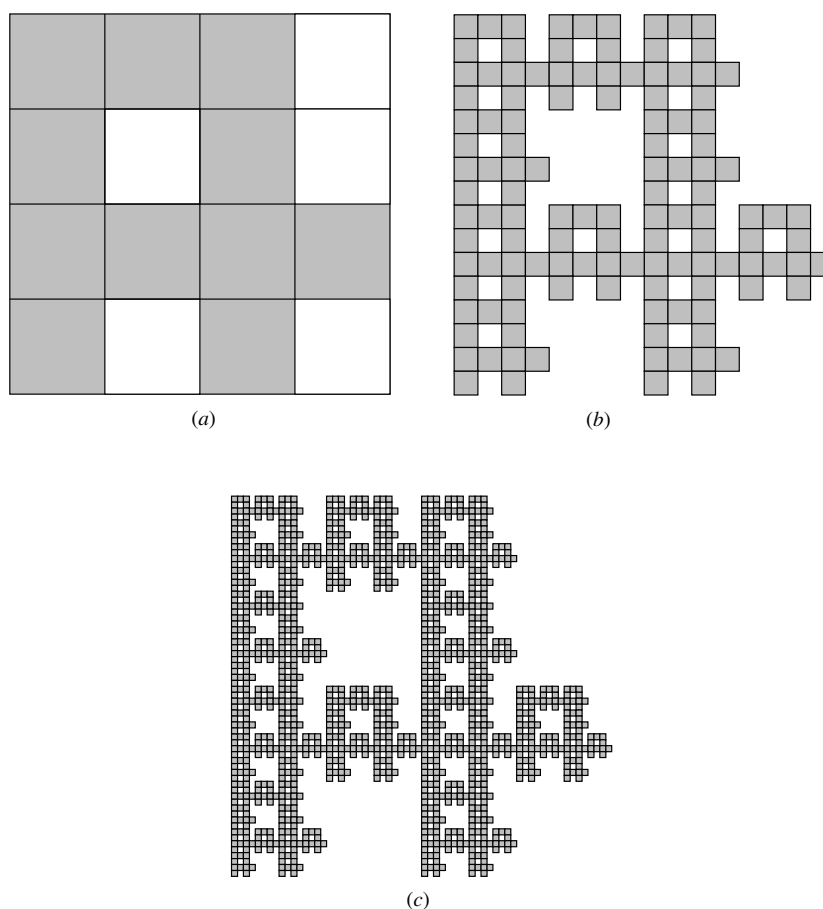


**Figure 1.** An example of a Sierpinski carpet generator (a) with  $n = 4$  and  $m = 11$  and the results of the second (b) and third (c) iterations of the construction procedure. Squares corresponding to white squares in the generator are removed.

$i$ th stage iterator are small dark and white squares, there is also no fractality for length scales less than the size of these small squares.

In a complementary case, where the pore is fractal, rather than the solid, one must identify the solid with phase 1 and the pore space as phase 2. In this case the porosity for the example carpet of figure 1 would be  $P_i = (11/16)^i$ , so that  $P_i \rightarrow 0$  as  $i \rightarrow \infty$ .

In modelling a real structure, a three-dimensional model would be more appropriate, but these ideas can easily be extended to three dimensions. In many cases, however, a two-dimensional section of the rock is studied as this is much simpler. In this case, the relative pore area intercepted by the section is termed as the ‘aerosity’. It is related to three-dimensional porosity and equals it in special cases [8].

### 3. Describing holes by vectors

Further on, we consider phase 1 as the pore space and phase 2, i.e. the dark squares, as the solid phase. Therefore, a hole in a Sierpinski carpet pattern is a cluster of white squares. We consider the white squares as being connected and thus belonging to the same

cluster if they have at least one vertex in common (they do not necessarily coincide at one edge). Note that this kind of connectivity is different from that defined for the dark squares in section 2.

An important quantity characterizing such a hole is the area, i.e. the number of white squares forming a cluster. These white squares have a size of  $n^{-2i}$  in the  $i$ th carpet stage. Counting the number of such squares corresponds to measuring the hole area in multiples of  $n^{-2i}$ . Furthermore, the size of the surface of a hole is important. Surface edges of a hole are all those bonds separating the hole cluster from the surrounding dark squares. They are of length  $n^{-i}$  in the  $i$ th carpet stage. Thus, counting the number of surface edges corresponds to measuring the surface in multiples of  $n^{-i}$ . Surface edges can be horizontal or vertical. Thus, we describe holes by a triple of integers

$$\underline{l} = \begin{pmatrix} \text{area} \\ \text{number of horizontal surface edges} \\ \text{number of vertical surface edges} \end{pmatrix}$$

further on called a *hole vector*. The area of a hole may also be zero, if the generator contains a pattern of four dark squares building up a square of twice the linear size. The corresponding hole vector is then  $(0, 0, 0)$ . All vectors considered here are column vectors, and also where denoted as row vectors (i.e. we skip the transposed sign in these cases).

To all the holes in the generator we assign a hole vector  $\underline{l}_i$  ( $i = 1, \dots, n_l$ ), where  $n_l$  denotes the number of holes. The only hole in the generator, shown in figure 1 for instance, is characterized by the hole vector  $\underline{l}_1 = (1, 2, 2)$ .

By a hole vector, not only holes, but also empty parts of the generator situated at the borders, which can combine to build a hole during the iteration, can be described. To achieve this we have to discuss the ramification of the fractal again.

Let us call the dark subsquares in which the first and last rows of the generator coincide and the dark subsquares in which the first and last columns of the generator coincide, *connecting* subsquares. With these squares a small copy of the generator contained in a higher iteration may be connected to neighbouring small copies of the generator. The connecting sites are marked with arrows in figure 2. Let  $r_h$  denote the number of connecting subsquares in the first (or last) row and  $r_v$  be the number of connecting subsquares in the first (or last) column of the generator. We call these numbers the *horizontal* and *vertical ramification*. Obviously, a Sierpinski carpet with  $r_h > 1$  or  $r_v > 1$  is *infinitely ramified*. For the example carpets shown in figure 2 one finds (a)  $r_h = 3$  and  $r_v = 3$ , and (b)  $r_h = 2$  and  $r_v = 1$ . Hence both carpets are infinitely ramified.

To every border part between two arrows a hole vector is assigned. The hole vectors for the corners are denoted with  $\underline{c}_1, \underline{c}_2, \underline{c}_3$  and  $\underline{c}_4$ , as shown in figure 2. For instance, the corner hole vector  $\underline{c}_1$  describes the number of white squares which are located between the leftmost  $\downarrow$  and the uppermost  $\rightarrow$  on the boundary of the generator and the horizontal and vertical edges between these two arrows (where the edges which the arrows refer to are not counted). For the generators in figure 2 we find  $\underline{c}_1 = (0, 0, 0)$  and  $\underline{c}_1 = (0, 0, 2)$ ; for example (a) and (b), respectively. Note that the vertical edges are marked with a thicker line in the latter case. These edges contribute to a potential hole as illustrated by the neighbouring generators in light grey.

If the Sierpinski carpet is infinitely ramified in the horizontal direction, then from left to right we have hole vectors  $\underline{h}_{iu}$  on the upper border (every one of these vectors describing the empty part of the generator between two successive  $\downarrow$ ) and analogously  $\underline{h}_{id}$  on the down border ( $i = 1, \dots, n_h = r_h - 1$ ). For the example carpet in figure 2(a) this definition yields  $\underline{h}_{1u} = \underline{h}_{1d} = \underline{h}_{2u} = \underline{h}_{2d} = (0, 0, 0)$  as the arrows are directly neighboured. On the other hand,

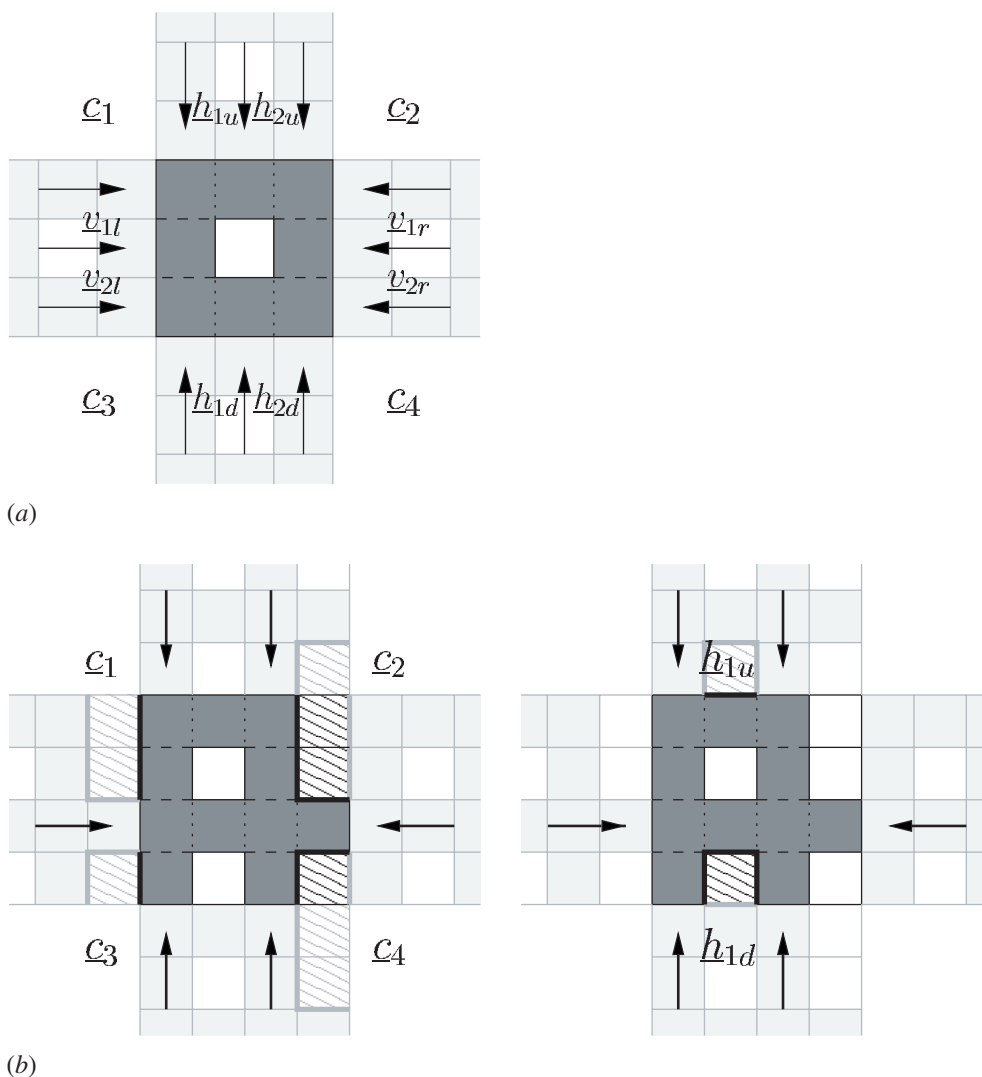


**Figure 2.** For (a) an easy and (b) our example generator (see figure 1) the connecting squares (denoted by arrows) and the border hole vectors ( $c_i, h_{iu}, h_{id}, v_{il}, v_{ir}$ ) are indicated. To clarify their contribution to the potential holes the corresponding edges and areas are highlighted and the neighbouring patterns are depicted in light grey. In addition, the horizontal (---) and vertical (···) edges between neighbouring dark sites are marked.

we find  $h_{1u} = (0, 1, 0)$  and  $h_{1d} = (1, 1, 2)$  for the example generator shown in figures 1 and 2(b).

The hole vectors  $h_{iu}$  and  $h_{id}$  will be combined with  $h_i = h_{iu} + h_{id}$  ( $i = 1, \dots, n_h$ ) describing the potential horizontal holes.

Analogously from top to bottom we get hole vectors  $v_{il}$  on the left border and  $v_{ir}$  on the right border and thus  $v_i = v_{il} + v_{ir}$  ( $i = 1, \dots, n_v = r_v - 1$ ) describing the potential vertical holes, if the fractal is infinitely ramified in the vertical direction. Combining these vectors

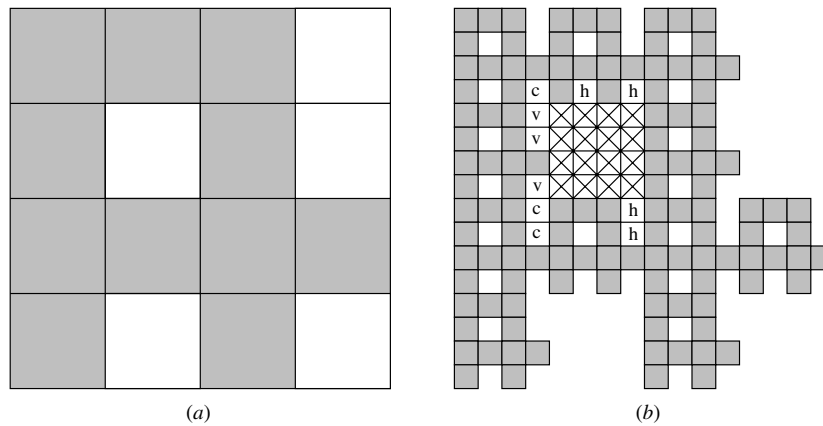


**Figure 3.** The hole of the example carpet generator (figure 1) is enlarged from the first to the second iteration, not only by decreasing the length scale, but also by the potential horizontal, vertical and corner holes.

we get

$$\underline{c} = \sum_{i=1}^4 \underline{c}_i \quad \text{potential corner hole}$$

$$\underline{h} = \underline{c} + \sum_{i=1}^{n_h} \underline{h}_i \quad \text{sum of potential horizontal holes and corner hole}$$

$$\underline{v} = \underline{c} + \sum_{i=1}^{n_v} \underline{v}_i \quad \text{sum of potential vertical holes and corner hole.}$$

With these definitions we find  $\underline{c}_1 = \underline{c}_2 = \underline{c}_3 = \underline{c}_4 = (0, 0, 0)$  and also  $n_h = n_v = 2$  with  $\underline{h}_1 = \underline{h}_2 = \underline{v}_1 = \underline{v}_2 = (0, 0, 0)$  for the example carpet (a) in figure 2. This yields  $\underline{c} = \underline{h} = \underline{v} = (0, 0, 0)$  for this easy example.

For the other example carpet shown in figures 1 and 2(b), we have in the horizontal direction  $n_h = 1$  with  $\underline{h}_1 = (1, 2, 2)$  and in the vertical direction  $n_v = 0$ . The corners are described by  $\underline{c}_1 = (0, 0, 2)$ ,  $\underline{c}_2 = (2, 1, 2)$ ,  $\underline{c}_3 = (0, 0, 1)$ ,  $\underline{c}_4 = (1, 1, 1)$  and thus  $\underline{c} = (3, 2, 6)$ . This results in  $\underline{h} = (4, 4, 8)$  and  $\underline{v} = (3, 2, 6)$ .

#### 4. Hole vectors under iteration

Now let us look at how a hole vector  $\underline{l} = (l_1, l_2, l_3)$  behaves under iteration. First of all, the area is multiplied by  $n^2$ , since an empty part of the unit square remains empty in the next iteration, but now we measure the area in multiples of squares contracted by a factor  $n$ . If we look, for instance, at the hole in our example generator (see figure 3(a)), these smaller squares are marked with  $\times$  in figure 3(b). Then an additional area is added on the borders: for every pair of horizontal edges we have to add the area of the potential horizontal holes and corner holes, i.e.  $h_1$ , and for every pair of vertical edges we have to add the area of the potential vertical holes and corner holes, i.e.  $v_1$ . Furthermore, some additional area occurs at the corners: this is exactly the area of the corner hole  $c_1$ . In figure 3(b), the corresponding small squares are marked with h, v and c, respectively. Thus, we get

$$l_1 \rightarrow n^2 l_1 + \frac{1}{2} l_2 h_1 + \frac{1}{2} l_3 v_1 + c_1 \quad (1)$$

for the area of the hole in the next iteration step.

Every edge is replaced by a set of smaller edges. For every pair of horizontal edges we get  $h_2$  smaller horizontal and  $h_3$  smaller vertical edges in the next iteration step surrounding the squares marked with  $h$  in figure 3(b). If such a surrounding edge is between a square marked with  $h$  and a square marked with  $\times$ , then this edge is, of course, not a border of the hole, but a corresponding border edge occurs on the opposite side of the hole between a square marked with  $\times$  and a dark square. Additionally,  $2r_h$  horizontal edges appear between dark squares and squares marked with  $\times$  connecting the other parts of the border. These edges correspond to the arrows in figure 2. Analogously, for every pair of vertical edges we get  $v_2$  smaller horizontal and  $v_3$  smaller vertical edges surrounding the squares marked with  $v$  and additionally  $2r_v$  vertical edges. The corner parts contribute  $c_2$  horizontal and  $c_3$  vertical edges surrounding the squares marked with  $c$ . Thus we get

$$\begin{aligned} l_2 &\rightarrow \frac{1}{2}l_2(2r_h + h_2) + \frac{1}{2}l_3v_2 + c_2 \\ l_3 &\rightarrow \frac{1}{2}l_2h_3 + \frac{1}{2}l_3(2r_v + v_3) + c_3. \end{aligned} \tag{2}$$

Combining (1) and (2) we define a function  $f$  describing how a hole vector evolves under the iteration:

$$\underline{f}(l) = \underline{M} \cdot l + \underline{c} \quad \text{with} \quad \underline{M} = \begin{pmatrix} n^2 & \frac{h_1}{2} & \frac{v_1}{2} \\ 0 & r_h + \frac{h_2}{2} & \frac{v_2}{2} \\ 0 & \frac{h_3}{2} & r_v + \frac{v_3}{2} \end{pmatrix}.$$

When iterating this equation we get

$$\underline{f}^i(l) = \underline{M}^i \cdot l + \left( \sum_{j=0}^{i-1} \underline{M}^j \right) \cdot \underline{c}$$

with

$$\underline{M}^j = \begin{pmatrix} \lambda_0^j & \frac{\lambda_0^j(h_3v_1 + h_1(2\lambda_0 - 2r_v - v_3))}{4(\lambda_0 - \lambda_1)(\lambda_0 - \lambda_2)} & \frac{\lambda_0^j(h_1v_2 + v_1(2\lambda_0 - 2r_h - h_2))}{4(\lambda_0 - \lambda_1)(\lambda_0 - \lambda_2)} \\ + \frac{\lambda_1^j(h_3v_1 + h_1(2\lambda_1 - 2r_v - v_3))}{4(\lambda_1 - \lambda_2)(\lambda_1 - \lambda_0)} & + \frac{\lambda_1^j(h_1v_2 + v_1(2\lambda_1 - 2r_h - h_2))}{4(\lambda_1 - \lambda_2)(\lambda_1 - \lambda_0)} \\ + \frac{\lambda_2^j(h_3v_1 + h_1(2\lambda_2 - 2r_v - v_3))}{4(\lambda_2 - \lambda_0)(\lambda_2 - \lambda_1)} & + \frac{\lambda_2^j(h_1v_2 + v_1(2\lambda_2 - 2r_h - h_2))}{4(\lambda_2 - \lambda_0)(\lambda_2 - \lambda_1)} \\ 0 & \frac{\lambda_1^j(2\lambda_1 - 2r_v - v_3) - \lambda_2^j(2\lambda_2 - 2r_v - v_3)}{2(\lambda_1 - \lambda_2)} & \frac{v_2(\lambda_1^j - \lambda_2^j)}{2(\lambda_1 - \lambda_2)} \\ 0 & \frac{h_3(\lambda_1^j - \lambda_2^j)}{2(\lambda_1 - \lambda_2)} & \frac{\lambda_1^j(2\lambda_1 - 2r_h - h_2) - \lambda_2^j(2\lambda_2 - 2r_h - h_2)}{2(\lambda_1 - \lambda_2)} \end{pmatrix}$$

where

$$\lambda_0 = n^2$$

$$\lambda_1 = \frac{h_2 + 2r_h + 2r_v + v_3 + \sqrt{(h_2 + 2r_h + 2r_v + v_3)^2 - 4(-h_3v_2 + (2r_h + h_2)(2r_v + v_3))}}{4}$$

$$\lambda_2 = \frac{h_2 + 2r_h + 2r_v + v_3 - \sqrt{(h_2 + 2r_h + 2r_v + v_3)^2 - 4(-h_3v_2 + (2r_h + h_2)(2r_v + v_3))}}{4}$$

are the eigenvalues of  $\underline{M}$ . For our example carpet (figure 1) the matrix  $\underline{M}$  has the special form

$$\underline{M} = \begin{pmatrix} 16 & 2 & 1.5 \\ 0 & 4 & 1 \\ 0 & 4 & 4 \end{pmatrix}$$



with the eigenvalues  $\lambda_0 = 16$ ,  $\lambda_1 = 6$  and  $\lambda_2 = 2$ ; hence we get

$$\underline{M}^j = \begin{pmatrix} 16^j & 3 \frac{16^j}{14} - \frac{6^j}{4} + \frac{2^j}{28} & \frac{16^j}{7} - \frac{6^j}{8} - \frac{2^j}{56} \\ 0 & \frac{6^j}{2} + \frac{2^j}{2} & \frac{6^j}{4} - \frac{2^j}{4} \\ 0 & 6^j - 2^j & \frac{6^j}{2} + \frac{2^j}{2} \end{pmatrix}.$$

Note that the eigenvalue  $\lambda_1$  can be used to calculate the scaling exponent  $d_p$  of the hole perimeter as we will discuss in section 7.

### 5. Hole-counting polynomial

To every iteration stage of the Sierpinski carpet we assign a hole-counting polynomial. This is a polynomial in three variables  $x$ ,  $y$  and  $z$ . Every hole, described by a hole vector  $\underline{l}$ , is characterized by a monomial  $x^{l_1} y^{l_2} z^{l_3}$ . The hole-counting polynomial  $p_i$  for the  $i$ th iteration of the Sierpinski carpet is then the sum of the monomials for all the holes in the  $i$ th stage.

Now we want to derive a recursive formula for the hole-counting polynomial of successive iterations of the Sierpinski carpet. Of course, the stage  $(i + 1)$  contains all the holes of the  $i$ th stage  $m$  times, thus  $p_{i+1}$  contains  $mp_i$ . Additionally, new holes appear by combining empty parts at the border of the  $i$ th iteration. There are different kinds of these new holes: first, every hole in the generator gives a larger new hole, whose hole vector can be derived by applying  $i$  times the function  $f$  to the original hole vector. Thus  $p_{i+1}$  contains  $\sum_{k=1}^{n_l} x^{f_1^i(l_k)} y^{f_2^i(l_k)} z^{f_3^i(l_k)}$ . Second, potential horizontal holes appear as holes on the  $s_h$  edges where  $i$ th stage carpets meet. These edges are denoted by dashed (---) lines for the example generators in figure 2. There we find  $s_h = 4$  and  $s_h = 6$  for examples (a) and (b), respectively. Each one of the  $n_h$  potential horizontal holes appears  $(i-1)$  times iterated, hence  $s_h \sum_{k=1}^{n_h} x^{f_1^{i-1}(h_k)} y^{f_2^{i-1}(h_k)} z^{f_3^{i-1}(h_k)}$  is contained in  $p_{i+1}$ . But in addition to these largest iterated potential horizontal holes, all smaller iterations appear and the number increases by a factor  $r_h$  with decreasing iteration. Thus, all new horizontal holes are described by the term  $s_h \sum_{k=1}^{n_h} \sum_{j=0}^{i-1} r_h^{i-j-1} x^{f_1^j(h_k)} y^{f_2^j(h_k)} z^{f_3^j(h_k)}$ . Third, an analogous term appears describing the new vertical holes:  $s_v \sum_{k=1}^{n_v} \sum_{j=0}^{i-1} r_v^{i-j-1} x^{f_1^j(v_k)} y^{f_2^j(v_k)} z^{f_3^j(v_k)}$ , where  $s_v$  is the number of vertical edges between neighbouring dark sites denoted by dotted ( $\cdots$ ) lines in figure 2.

So iteratively we can get the hole-counting polynomial by

$$\begin{aligned} p_{i+1}(x, y, z) &= m \cdot p_i(x, y, z) + \sum_{k=1}^{n_l} x^{f_1^i(l_k)} y^{f_2^i(l_k)} z^{f_3^i(l_k)} \\ &+ s_h \sum_{k=1}^{n_h} \sum_{j=0}^{i-1} r_h^{i-j-1} x^{f_1^j(h_k)} y^{f_2^j(h_k)} z^{f_3^j(h_k)} \\ &+ s_v \sum_{k=1}^{n_v} \sum_{j=0}^{i-1} r_v^{i-j-1} x^{f_1^j(v_k)} y^{f_2^j(v_k)} z^{f_3^j(v_k)}. \end{aligned} \tag{3}$$

Obviously, the polynomial  $p_1$  describing the generator has the form

$$p_1(x, y, z) = \sum_{k=1}^{n_l} x^{l_k} y^{l_k} z^{l_k}.$$

We also get this polynomial by applying the iteration formula (3) starting with  $p_0(x, y, z) = 0$ . So the starting point of the iteration formula can be given in the simple form  $p_0 = 0$ .

For the example carpet shown in figure 1, the recursive formula for the hole-counting polynomials is

$$p_{i+1}(x, y, z) = 11p_i(x, y, z) + x^{f_1^i((1,2,2))}y^{f_2^i((1,2,2))}z^{f_3^i((1,2,2))} + 6 \sum_{j=0}^{i-1} 2^{i-j-1}x^{f_1^j((1,2,2))}y^{f_2^j((1,2,2))}z^{f_3^j((1,2,2))}.$$

The first iterations for this example give

$$\begin{aligned} p_0 &= 0 \\ p_1 &= x^1y^2z^2 \\ p_2 &= 11x^1y^2z^2 + x^{26}y^{12}z^{22} + 6x^1y^2z^2 \\ &= 17x^1y^2z^2 + x^{26}y^{12}z^{22} \\ p_3 &= 187x^1y^2z^2 + 11x^{26}y^{12}z^{22} + x^{476}y^{72}z^{142} + 6 \cdot 2x^1y^2z^2 + 6x^{26}y^{12}z^{22} \\ &= 199x^1y^2z^2 + 17x^{26}y^{12}z^{22} + x^{476}y^{72}z^{142} \\ &\vdots \end{aligned}$$

This especially means that the generator contains one hole of size 1 with two horizontal and two vertical border edges and the second iteration of this carpet contains 17 such small holes and additionally one hole of size 26 with 12 horizontal and 22 vertical edges, as can easily be checked in figure 1.

### 6. Special case: finitely ramified carpets

As explained in section 3, finitely ramified Sierpinski carpets are characterized by  $r_h = 1$  and  $r_v = 1$ . Furthermore, there are no potential horizontal and vertical holes, i.e.  $\underline{h} = \underline{v} = \underline{c}$ . Since there is no difference between the vectors  $\underline{h}$  and  $\underline{v}$ , it is not important to distinguish between horizontal and vertical edges any more. Thus we can reduce the hole vectors to two-dimensional vectors

$$\tilde{\underline{l}} = \begin{pmatrix} \text{area} \\ \text{number of surface edges} \end{pmatrix}.$$

Specifically, we get a two-dimensional vector  $\tilde{\underline{c}}$  describing the potential corner hole.

The function  $\tilde{f}$  describing how a hole vector evolves under the iteration then has the special form

$$\tilde{f}(\tilde{\underline{l}}) = \tilde{\underline{M}} \cdot \tilde{\underline{l}} + \tilde{\underline{c}} \quad \text{with} \quad \tilde{\underline{M}} = \begin{pmatrix} n^2 & \frac{\tilde{c}_1}{2} \\ 0 & 1 + \frac{\tilde{c}_2}{2} \end{pmatrix}.$$

Since the number of potential horizontal and vertical holes is zero, the iteration formula for the hole-counting polynomials has the simple form

$$\tilde{p}_{i+1}(x, y) = m\tilde{p}_i(x, y) + \sum_{k=1}^{n_i} x^{\tilde{f}_1^i(\tilde{\underline{l}}_k)}y^{\tilde{f}_2^i(\tilde{\underline{l}}_k)} \tag{4}$$

again starting with  $\tilde{p}_0 = 0$ , where the exponent for  $y$  is the whole number of edges.

Now let us consider the iteration  $\tilde{f}^i$  in more detail. As in the general case we have

$$\tilde{f}^i(\tilde{\underline{l}}) = \tilde{\underline{M}}^i \cdot \tilde{\underline{l}} + \left( \sum_{j=0}^{i-1} \tilde{\underline{M}}^j \right) \cdot \tilde{\underline{c}}.$$

This equation can be simplified using the relations  $\left(\sum_{j=0}^{i-1} \underline{\tilde{M}}^j\right) \cdot \underline{\tilde{c}} = \underline{\tilde{f}}^{i-1}(\underline{\tilde{c}})$  and  $\underline{\tilde{f}}_2^{i-1}(\underline{\tilde{c}}) = \underline{\tilde{c}}_2 \sum_{j=0}^{i-1} \left(1 + \frac{\underline{\tilde{c}}_2}{2}\right)^j = 2\left(1 + \frac{\underline{\tilde{c}}_2}{2}\right)^i - 2$ . This results in

$$\underline{\tilde{f}}^i(\underline{\tilde{l}}) = \begin{pmatrix} n^{2i} & \frac{1}{2} \underline{\tilde{f}}_1^{i-1}(\underline{\tilde{c}}) \\ 0 & \left(1 + \frac{\underline{\tilde{c}}_2}{2}\right)^i \end{pmatrix} \underline{\tilde{l}} + \begin{pmatrix} \underline{\tilde{f}}_1^{i-1}(\underline{\tilde{c}}) \\ 2\left(1 + \frac{\underline{\tilde{c}}_2}{2}\right)^i - 2 \end{pmatrix}. \quad (5)$$

Hence the evolution of any hole under the iteration of  $\underline{\tilde{f}}$  is fully described by the evolution of the area of the potential corner hole.

Since there are no potential horizontal and vertical holes in a finitely ramified Sierpinski carpet, the area of the  $(i - 1)$  times iterated potential corner hole can also be determined in another way: this area is the whole area of the  $i$  times iterated carpet,  $n^{2i}$ , minus the number of dark sites,  $m^i$ , minus the number of sites situated in any hole. The sum of the areas of all the holes can simply be derived from the hole-counting polynomial  $\tilde{p}_i$ : it is the sum over all the  $x$ -exponents times the coefficients, i.e.  $\frac{\partial}{\partial x} \tilde{p}_i(1, 1)$ . Thus we get

$$\underline{\tilde{f}}_1^{i-1}(\underline{\tilde{c}}) = n^{2i} - m^i - \frac{\partial}{\partial x} \tilde{p}_i(1, 1). \quad (6)$$

Inserting (5) and (6) in (4) gives the iteration formula of the hole-counting polynomial for finitely ramified Sierpinski carpets in the following form:

$$\tilde{p}_{i+1}(x, y) = m \tilde{p}_i(x, y) + \sum_{k=1}^{n_i} x^{n^{2i} \tilde{l}_{k1} + \left(\frac{\tilde{l}_{k2}}{2} + 1\right)} (n^{2i} - m^i - \frac{\partial}{\partial x} \tilde{p}_i(1, 1)) y^{\left(1 + \frac{\underline{\tilde{c}}_2}{2}\right)^i \tilde{l}_{k2} + 2 \left(1 + \frac{\underline{\tilde{c}}_2}{2}\right)^i - 2}.$$

## 7. Dimensions extracted from the polynomial

The hole-counting polynomial can be used, for example, to find a suitable Sierpinski carpet in a reasonable iteration depth to model porous media. If a low iteration depth is considered the hole sizes and perimeters in the carpet and porous material can be compared directly. If one is not interested in the number of holes of a certain size alone, the scaling properties of the hole area and the perimeter with respect to the linear length of the fractal can also be analysed.

In an infinitely iterated Sierpinski carpet there are sequences of similar holes. The largest hole of such a sequence corresponds to a hole in the generator where at the border some new area is added during the iteration. Resulting from the self-similarity, such a hole occurs  $m$  times scaled down by a factor  $1/n$ , every one of these smaller holes again occurs  $m$  times scaled down by a factor  $1/n$ , and so on. Hence, in a log–log plot of the number of holes over the linear size for every hole in the generator, we would get a straight line with slope

$$\frac{\log(m)}{\log(1/n)} = -\frac{\log(m)}{\log(n)} = -d_f.$$

For infinitely ramified carpets, in every iteration new hole sequences start resulting from the potential horizontal and vertical holes. These sequences, of course, show the same behaviour during the iteration. Since the size of the starting holes is the same in every iteration, these different sequences cannot be distinguished in a log–log plot of the number of holes over the linear size.

The exponents in the hole-counting polynomial describe the area and the perimeter (sum of horizontal and vertical surface edges) of the holes. Let us first analyse the number of holes of a certain area. Figure 5 shows a log–log plot of the number of holes over the hole area for two different iterations of the Sierpinski carpet shown in figure 4. This carpet generator (figure 4(a)) has holes and potential holes of different sizes. For a small iteration number, the different hole sequences can be noted (figure 5(a)), whereas for large enough iterations

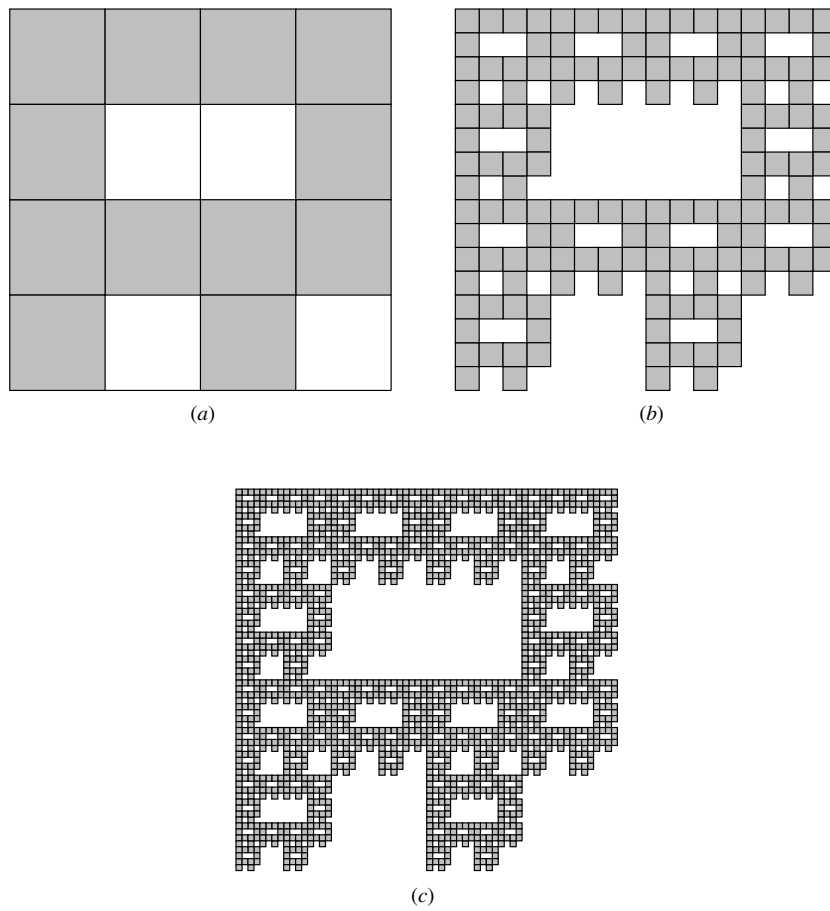


**Figure 4.** An example of a Sierpinski carpet generator (a) with holes and potential holes with different areas, which results in different holes in the second (b) and third (c) iterations.

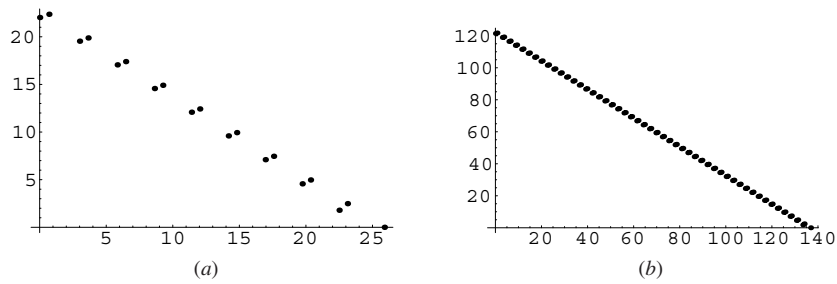


**Figure 5.** Log-log plot of the number of holes over the hole area for iterations 10 (a) and 50 (b).

the data points are nearly on a straight line (figure 5(b)). Thus for high iterations a straight line can be fitted through the data points. The slope of this line is  $-d_f/2$ . As explained above, resulting from the self-similarity every hole occurs  $m$  times scaled down by a factor  $1/n$ . Since

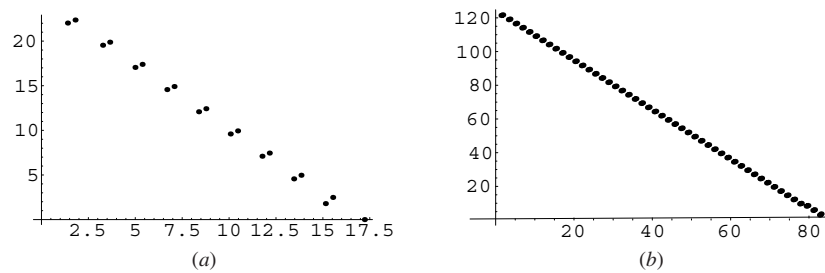


**Figure 6.** Log–log plot of the number of holes over the hole perimeter for iterations 10 (a) and 50 (b) for the carpet shown in figure 4.

the horizontal axis in figure 5 is the area of the hole, this quantity scales down by a factor  $1/n^2$ . Thus a slope of

$$\frac{\log(m)}{\log(1/n^2)} = -\frac{\log(m)}{2 \log(n)} = -\frac{d_f}{2} \quad (7)$$

follows. The exponent 2 in the denominator of the first term of (7) indicates that the hole area is two dimensional. Hence the quantity  $d_a = -d_f/\text{slope} = 2$  gives the dimension of the hole area. For our example carpet the linear fit for iteration 100 gives the estimate  $d_a = 2.00092$  for the dimension of the hole area.

Now the question arises: what slope will a log–log plot of the number of holes over the perimeter give? This number results in an estimate  $d_p = -d_f/\text{slope}$  of the dimension of the hole perimeter. The lower limit for  $d_p$  is 1 and the upper limit is  $d_f$ , because the hole perimeter is a subset of the whole Sierpinski carpet. This situation can be compared to the discussion on holes in a percolation cluster [9] where the hole perimeter is the ‘lake front’ and the external boundary is the ‘ocean front’ on a fractal island. It must be emphasized that  $d_p$  here is the scaling exponent for the perimeter of a single hole, not the sum of the perimeters for all the holes, which must, of course, scale as  $d_f$ .

Figure 6 shows a log–log plot of the number of holes over the hole perimeter for two different iterations of the Sierpinski carpet shown in figure 4. As for the hole area (see figure 5), for small iteration numbers different hole sequences can be noted, whereas for large iterations all data points are nearly on a straight line. The absolute value of the slope of this line is larger compared with figure 5. From figure 6(b) the dimension of the hole perimeter can be estimated as  $d_p = 1.21907$ . This is indeed a number between 1 and 2.

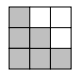
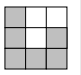
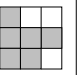
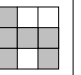
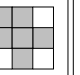
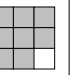
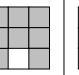
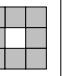
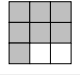
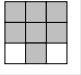
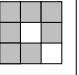
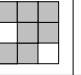
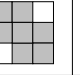
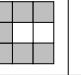
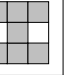
The perimeter dimension can also be calculated directly from the matrix  $\underline{\underline{M}}$  discussed in section 4. Consider the sub-matrix

$$\underline{\underline{M}}^* = \begin{pmatrix} M_{22} & M_{23} \\ M_{32} & M_{33} \end{pmatrix} = \begin{pmatrix} r_h + \frac{h_2}{2} & \frac{v_2}{2} \\ \frac{h_3}{2} & r_v + \frac{v_3}{2} \end{pmatrix}$$

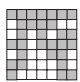
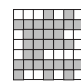
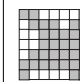
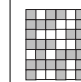
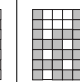
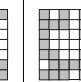
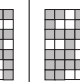
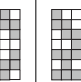
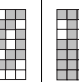
which describes how the horizontal and vertical edges of the holes evolve under the iteration. For high enough iterations the number of edges in the next iteration is determined simply by multiplying the actual number with the largest eigenvalue of the matrix  $\underline{\underline{M}}^*$ , which is that denoted by  $\lambda_1$  in section 4. Therefore, the exponent  $d_p$ , which describes the scaling of both types of edges with the linear length of the carpet, is given by  $d_p = \log(\lambda_1)/\log(n)$ . For the example carpet in figure 4 we find  $d_p = \log(4 + \sqrt{2})/\log(4) = 1.21838$ , which is in good agreement with the result from the hole-counting polynomial.

Table 1 shows all possible  $3 \times 3$  Sierpinski carpet generators with holes and three different dimensions: the fractal dimension, the dimension of the hole perimeter calculated from the

**Table 1.** For all possible  $3 \times 3$  Sierpinski carpet generators with holes the fractal dimension  $d_f$ , the dimension  $d_p$  of the hole perimeter and the random walk dimension  $d_w$  are shown.

								
$d_f$	1.631	1.631	1.631	1.631	1.631	1.893	1.893	1.893
$d_p$	1.465	1.562	1.465	1.562	1.465	1.262	1.000	1.000
$d_w$	2.545	2.564	2.545	2.560	2.545	2.192	2.116	2.095
								
$d_f$	1.771	1.771	1.771	1.771	1.771	1.771	1.771	
$d_p$	1.352	1.352	1.631	1.562	1.465	1.000	1.000	
$d_w$	2.229	2.218	2.557	2.559	2.543	2.146	2.136	

**Table 2.** For some infinitely ramified  $7 \times 7$  Sierpinski carpet generators with holes, the dimensions  $d_f$ ,  $d_p$  and  $d_w$  are shown.

									
$d_f$	1.748	1.748	1.748	1.748	1.748	1.748	1.748	1.748	1.748
$d_p$	1.318	1.377	1.183	1.443	1.226	1.381	1.392	1.507	1.456
$d_w$	2.320	2.372	2.275	2.396	2.281	2.345	2.360	2.552	2.489

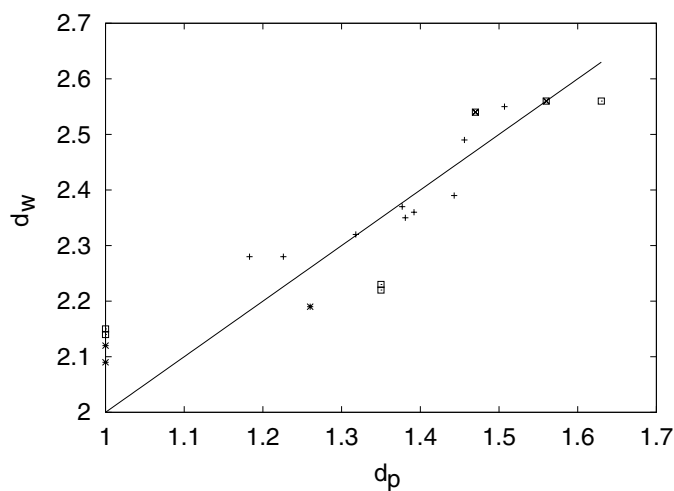


**Figure 7.** For all the carpets shown in tables 1 and 2 the random walk dimension  $d_w$  is plotted over the dimension of the hole perimeter  $d_p$ , together with the straight line  $d_w = d_p + 1$ . Identical symbols correspond to carpets with the same fractal dimension: ( $\times$ )  $d_f = 1.631$ , ( $+$ )  $d_f = 1.748$ , ( $\square$ )  $d_f = 1.771$ , ( $*$ )  $d_f = 1.893$ .

largest eigenvalue of  $\underline{M}^*$  and the random walk dimension. The random walk dimension is determined by the resistance-scaling algorithm [10] for the finitely ramified carpets and by the algorithm of [11] for 500 000 random walks of length 10 000 for the infinitely ramified ones. In table 2 the same dimensions are given for the nine infinitely ramified  $7 \times 7$  generators considered in [11].

All considered generators in tables 1 and 2 that yield carpets with the same  $d_f$  and  $d_p$  have nearly the same random walk dimension. So there may be a dependence of  $d_w$  on  $d_f$  and  $d_p$ . Therefore we plotted  $d_w$  over  $d_p$  for all the  $3 \times 3$  and  $7 \times 7$  carpets (figure 7). Our expectation was that for carpets with the same  $d_f$ , the larger  $d_p$  was the larger  $d_w$  would be, because the more compact a hole of a given area is, the less it hinders the random walk. This expectation is approximately confirmed in figure 7. Apart from some fluctuations there is a monotonic dependence of  $d_w$  on  $d_p$ ; it even seems not to be influenced by  $d_f$ . The straight line in figure 7 is given by  $d_w = d_p + 1$ . Although this relationship is not exactly fulfilled,  $d_p + 1$  seems to be a good approximation for  $d_w$ .

## 8. Conclusions

In this paper we have derived a new method for investigating the pore structure of Sierpinski carpets. The hole distribution for every iteration of the carpet can be described by a hole-counting polynomial, and for this polynomial an iterative formula is given. This polynomial contains all information about the holes in every stage and especially the dimension of the hole area and the hole perimeter for the infinitely iterated carpet. Whereas the hole area is known to be two dimensional, the dimension of the hole perimeter  $d_p$  is a new dimension characterizing the pore structure of the Sierpinski carpets, which to our knowledge has never been investigated before.

Since a random walker on fractal lattices has to move around the holes, the dimension of the hole perimeter should be related to the random walk dimension  $d_w$ . For the example carpets investigated in this paper,  $d_w$  differs by at most 0.2 from  $d_p + 1$ . This is important, since an accurate approximation of  $d_w$  for infinitely ramified Sierpinski carpets requires simulating a huge number of long random walks, which is computationally very expensive, whereas  $d_p$  can be calculated analytically from the generator. There is as yet no exact relation connecting the dynamic exponent  $d_w$  with static exponents, such as  $d_f$  and  $d_l$  (the chemical dimension), as is available for loopless carpets with finite ramification [12]. It may seem surprising that the approximate expression for  $d_w$  does not involve  $d_f$ , but indirectly  $d_p$  does contain information about  $d_f$ , i.e. the number of white squares in the generator as well as their arrangement. It also has the correct limits. The lower limit gives  $d_w = 2$ , valid for normal diffusion, and the upper limit is  $d_w = 1 + d_f$ , which is true for loopless patterns with  $d_f = d_l$  [12].

It is an interesting question whether the relation between  $d_w$  and  $d_p$  is confined to Sierpinski carpets. Hence a subject of further research is the extension of the hole-counting polynomial to a wider class of fractals such as, for instance, the invariant sets of more general iterated function systems. Algorithms for computing  $d_p$  analogous to those shown in this paper could also be developed for this more general case.

Of course, the relation  $d_w \approx d_p + 1$  is just a rough approximation. The deviations from the straight line in figure 7 are not only due to numerical inaccuracies of the  $d_w$  values caused by the finite length and number of the considered walks. For the finitely ramified Sierpinski carpets we know  $d_w$  up to an arbitrary accuracy by the resistance-scaling method. So if the relation  $d_w \approx d_p + 1$  was exactly fulfilled, the data points for the finitely ramified carpets should at least lie on the straight line in figure 7 but obviously they do not. Hence finding an exact dependence of the random walk dimension on  $d_f$  and  $d_p$ , but maybe also on other dimensions

such as the chemical dimension  $d_b$ , is a topic of further research. The new exponent  $d_p$  is likely to be important for the study of rocks where the interface is sometimes found to scale differently from the mass fractal dimension.

Details of various Sierpinski carpets have been studied by a transfer matrix method [13, 14]. Here the carpet consists of ‘bonds’ and removal of a subsquare removes the bonds bounding it. This results in different types of subsquares in the next stage with one or more open sides. The open sides of the squares correspond to the pore–solid interface in our case. So there are points of similarity in the two approaches. It would be interesting to see whether the eigendimensions obtained by [13] are related to  $d_p$ .

## References

- [1] Bunde A and Havlin S (ed) 1996 *Fractals and Disordered Systems* (Berlin: Springer)
- [2] Adler P M 1986 *Phys. Fluids* **29** 15
- [3] Roy S, Dasgupta R and Tarafdar S 1996 *Solid State Ionics* **86–88** 363
- [4] Roy S and Tarafdar S 1997 *Phys. Rev. B* **55** 8038
- [5] Falconer K J 1997 *Techniques in Fractal Geometry* (Chichester: Wiley)
- [6] Seeger S, Franz A, Schulzky C and Hoffmann K H 2000 *Comput. Phys. Commun.* **134** 307
- [7] Tarafdar S, Franz A, Schulzky C and Hoffmann K H 2000 *Physica A* **292** 1
- [8] Clennel M B 1997 *Developments in Petrophysics (Geological Society Special Publication 122)* ed M A Lovell and P K Harvey, p 299
- [9] Stanley H E 1986 *On Growth and Form; Fractal and Non-Fractal Patterns in Physics* ed H E Stanley and N Ostrowsky, p 21
- [10] Schulzky C, Franz A and Hoffmann K H 2000 *SIGSAM Bull.* **34** 1
- [11] Dasgupta R, Ballabh T K and Tarafdar S 1999 *J. Phys. A: Math. Gen.* **32** 6503
- [12] Havlin S and Ben-Avraham D 1987 *Adv. Phys.* **36** 695
- [13] Mandelbrot B, Gefen Y, Aharony A and Peyriere J 1985 *J. Phys. A: Math. Gen.* **18** 335
- [14] Perreau M and Levy J C S 1989 *Phys. Rev. A* **40** 4690